Molecular Cell, Vol. 13, 639–648, March 12, 2004, Copyright ©2004 by Cell Press

Structural Basis for the Mechanism and Regulation of Sir2 Enzymes

José L. Avalos,[1] Jef D. Boeke,[2] and Cynthia Wolberger[1,3,*]
[1]Department of Biophysics and Biophysical Chemistry
[2]Department of Molecular Biology and Genetics
[3]Howard Hughes Medical Institute
Johns Hopkins University School of Medicine
725 North Wolfe Street
Baltimore, Maryland 21205

Summary

Sir2 proteins form a family of NAD^+-dependent protein deacetylases required for diverse biological processes, including transcriptional silencing, suppression of rDNA recombination, control of p53 activity, regulation of acetyl-CoA synthetase, and aging. Although structures of Sir2 enzymes in the presence and absence of peptide substrate or NAD^+ have been determined, the role of the enzyme in the mechanism of deacetylation and NAD^+ cleavage is still unclear. Here, we present additional structures of Sir2Af2 in several differently complexed states: in a productive complex with NAD^+, in a nonproductive NAD^+ complex with bound ADP-ribose, and in the unliganded state. We observe a new mode of NAD^+ binding that seems to depend on acetyl-lysine binding, in which the nicotinamide ring of NAD^+ is buried in the highly conserved "C" pocket of the enzyme. We propose a detailed structure-based mechanism for deacetylation and nicotinamide inhibition of Sir2 consistent with mutagenesis and enzymatic studies.

Introduction

The Sir2 family of proteins, also known as sirtuins, are protein deacetylases that play critical roles in diverse biological processes, including transcriptional silencing (Braunstein et al., 1993), aging (Kaeberlein et al., 1999; Lin et al., 2000; Tissenbaum and Guarente, 2001), suppression of rDNA recombination (Gottlieb and Esposito, 1989), transcriptional regulation (Fulco et al., 2003), and deacetylation of the p53 tumor suppressor (Luo et al., 2001; Vaziri et al., 2001), the pol I transcription factor TAF_I68 (Muth et al., 2001), acetyl-coA synthetase (Starai et al., 2002), and tubulin (North et al., 2003). These highly conserved enzymes, which are found in organisms of all three domains of life, deacetylate lysine residues in a unique reaction that consumes NAD^+, releasing nicotinamide, *O*-acetyl ADP ribose, and the deacetylated product (Imai et al., 2000; Landry et al., 2000; Smith et al., 2000; Tanner et al., 2000; Tanny and Moazed, 2001). In addition to the dependence of enzyme activity on the concentration of free NAD^+, sirtuin activity can also be regulated by the reaction product nicotinamide, a potent noncompetitive inhibitor of some sirtuins proposed to control Sir2 activity in vivo (Anderson et al., 2003; Bitterman et al., 2002). The complex chemistry by which sirtuins deacetylate acetyl-lysine—a reaction that other classes of histone deacetylases carry out by simple hydrolysis—may allow regulation of the deacetylation reaction in response to other cellular signals.

The mechanism by which sirtuins catalyze NAD^+-dependent deacetylation of lysine residues has been the focus of biochemical and structural studies. Isotope labeling experiments suggest that the reaction proceeds through a nucleophilic attack on the C1′ of the nicotinamide ribose, leading to formation of a metastable covalent intermediate between ADP-ribose and acetyl-lysine, with concomitant release of nicotinamide (Sauve et al., 2001). The subsequent steps in the reaction lead to formation of the deacetylated peptide and a mixture of 2′- and 3′-*O*-acetyl-ADP ribose. If free nicotinamide binds to the enzyme containing the covalent intermediate, a base exchange reaction may occur, leading to reformation of NAD^+ and release of the acetylated peptide (Jackson et al., 2003; Sauve and Schramm, 2003). Crystal structures of archaeal (Avalos et al., 2002; Chang et al., 2002; Min et al., 2001) and eukaryotic (Finnin et al., 2001; Zhao et al., 2003a, 2003b) sirtuins have shown that the enzyme contains a cleft where the substrates and reaction products bind. The cleft separates a large Rossmann fold domain from a smaller domain that is composed of a zinc binding module and a flexible helical subdomain (Min et al., 2001) (Figure 1A). Structures of *Archaeoglobus fulgidus* Sir2Af2 (Avalos et al., 2002) and of yeast Hst2 (Zhao et al., 2003b) bound to acetylated peptide show that the acetyl-lysine inserts into a hydrophobic tunnel, placing the acetyl group adjacent to the NAD^+ binding site. Structures of a second *A. fulgidus* enzyme, Sir2Af1, have been determined in complex with NAD^+ (Min et al., 2001). Since the nicotinamide ring was disordered in both reported structures, the location of the nicotinamide was inferred from the position of the nicotinamide ribose (N-ribose). Although these structures share a common mode of binding for the adenine nucleoside, the position of the N-ribose and the inferred position of the nicotinamide differ between them (Figure 1B), suggesting a large conformational flexibility of the nicotinamide moiety. Moreover, the previously observed conformations of NAD^+ fail to account for the invariance of key residues required for enzymatic activity (Armstrong et al., 2002; Chang et al., 2002; Imai et al., 2000; Min et al., 2001) and place the nicotinamide ring in positions incompatible with acetyl-lysine binding (Avalos et al., 2002). As a consequence, it has until now been impossible to propose a detailed structure-based mechanism for the deacetylation and nicotinamide exchange reactions consistent with biochemical data.

To help determine the role of sirtuins in the enzymatic mechanism, we have solved five structures of Sir2Af2 in differently liganded states. Three of the complexes contain completely ordered bound NAD^+. Moreover, the NAD^+ in two of these complexes is bound in a newly observed conformation that places the nicotinamide ring in direct contact with many invariant residues. In

*Correspondence: cwolberg@jhmi.edu

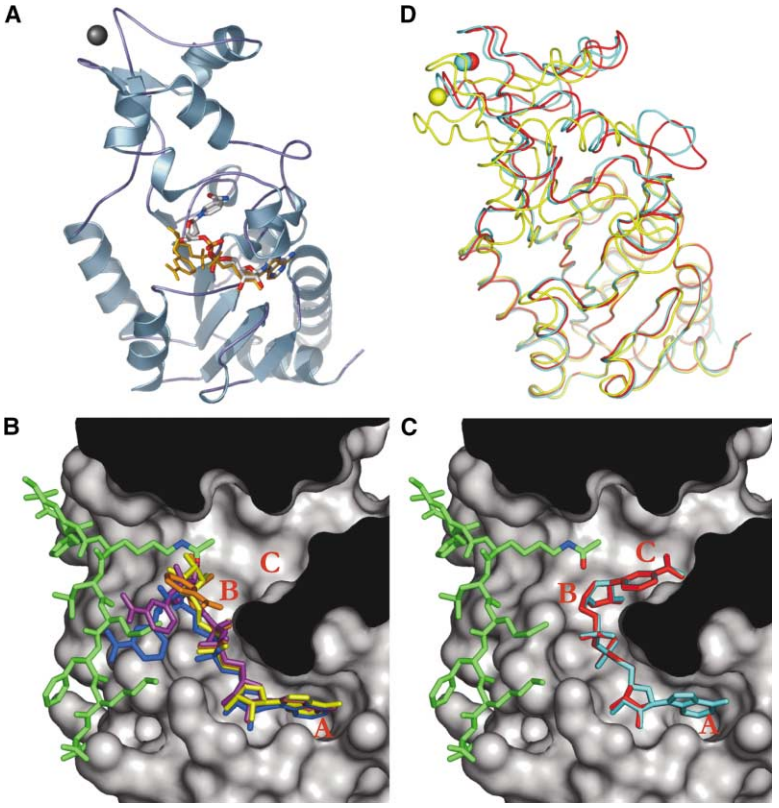

Figure 1. Structures of Archaeal Sir2 Bound to NAD^+ and ADP-Ribose

(A) Cartoon diagram of a productive Sir2Af2-NAD^+ complex with the NAD^+ in atom colors. The superimposed NAD^+ conformation from the nonproductive complex is shown in yellow.

(B) The active site of Sir2Af2 with the superimposed structures of acetylated peptide (green), ADP ribose (yellow), and nonproductive NAD^+ bound to Sir2Af2 (blue). The structures of the nonproductive NAD^+ molecules bound to Sir2Af1 are also shown (orange and purple). The A, B, and C pockets of Sir2Af2 are labeled in red.

(C) The superimposition of the two NAD^+ molecules observed in a productive conformation (cyan and red) with the structure of the acetylated peptide (green). A proposed nicotinamide exit channel toward the opposite side of the enzyme is shown.

(D) Structures of Sir2Af2 superimposed show significant conformational differences in the small domain (only three are shown for simplicity). The figure shows the ribbon diagram of the backbones of Sir2Af2 in complex with NAD^+ in the productive conformation (red and cyan), which superimpose very well with each other, and with ADP-ribose (yellow), which deviates significantly in the conformation of the small domain. The ligands have been removed for simplicity.

this conformation, the ground state of NAD^+ is destabilized by straining the planarity of the nicotinamide moiety and burying the charge of the NAD^+ in a largely hydrophobic environment. This NAD^+ conformation is compatible with an acetyl-lysine attack on the N-ribose (Figure 1C). This productive complex with NAD^+ appears to be promoted by a PEG molecule fortuitously bound in the acetyl-lysine binding tunnel, suggesting that binding of the acetylated peptide substrate positions NAD^+ for catalysis. A third Sir2Af2-NAD^+ complex that lacks a peptide substrate mimic contains a less well-ordered NAD^+ molecule in a different conformation that is incompatible with peptide binding (Figure 1B). We also describe the structure of a complex with ADP-ribose, as well as the structure of the Sir2Af2 apo-enzyme (Figures 1B and 1D). In addition, these structures shed light on the mechanism of nicotinamide exchange in sirtuins, which is essential for their regulation by this product. Together with the previously reported structure of Sir2Af2 bound to an acetylated peptide, these structures allow us to propose a structure-based mechanism involving ground state destabilization of NAD^+ that is consistent with enzymatic studies and accounts for the conservation of invariant residues of previously unknown function.

Results

Overview of the Sir2Af2 Complex Structures

The four structures of differently liganded Sir2Af2 proteins were determined from a single crystal of Sir2Af2 grown in the presence of NAD^+ and PEG 400 (see Experimental Procedures). The crystals, which form in the space group $P2_12_12$, contain five molecules in the asymmetric unit. Two of the complexes are nearly identical in protein conformation (Figure 1D) and contain ordered NAD^+ bound in an identical conformation (Figure 1C). These complexes also contain bound PEG within the acetyl-lysine binding tunnel and, for reasons described more fully below, are referred to as productive complexes. Another complex with NAD^+ that lacks PEG in the acetyl-lysine binding tunnel contains a fully ordered NAD^+ molecule bound in a different conformation that is incompatible with acetyl-lysine binding (Figure 1B). This complex, which we call the nonproductive complex, also differs from the productive complexes in the relative position and conformation of the small domain. Another complex in the crystal contains bound ADP-ribose (Figure 1B), which presumably derives from hydrolyzed NAD^+ in the crystallization drops. The electron density clearly indicates the presence of the α anomer of the ribose ring, consistent with the hydrolysis of the β NAD^+ used in the crystallization. α-ADP ribose has also been found in crystals of Sir2Af1 that grew in the presence of NAD^+ (Chang et al., 2002) and is likely also present in a recently reported complex with Hst2 (Zhao et al., 2003b). The fifth molecule in the asymmetric unit lacks any bound substrate. The five Sir2Af2 proteins reported here were built independently and refined without noncrystallographic symmetry restraints to an R/R_{free} of 20.7%/25.0% at 2.3 Å resolution. The superposition of all structures of Sir2Af2 shows significant conformational flexibility in the small domain (Figure 1D), which we address below.

Productive Complexes with NAD^+

Two of the Sir2Af2-NAD^+ complexes contain NAD^+ bound in a previously unreported conformation that appears to be favored by the binding of a substrate mimic. The fully ordered NAD^+ molecule binds in a manner that buries the nicotinamide ring in a conserved site called the "C" pocket (Min et al., 2001) (Figures 1C and 2A), thereby placing the nicotinamide ring and N-ribose in direct contact with invariant and catalytically important residues (Figures 2A and 2B). These complexes also have in common a bound PEG molecule that binds within the acetyl-lysine binding tunnel, thereby mimicking substrate binding (Figure 2C). The superposition of this NAD^+ complex with the structure of Sir2Af2 bound to acetylated peptide (Avalos et al., 2002) shows that this conformation of NAD^+ is fully compatible with simultaneous binding of acetyl-lysine (Figure 1C). This superposition also places the C1′ atom of the N-ribose about 2.8 Å from the carbonyl oxygen of acetyl-lysine (Figure 2A). The acetyl-lysine approaches the N-ribose at the α face, consistent with isotope labeling experiments that suggest an initial attack by the carbonyl oxygen of the acetyl group on the C1′ of the N-ribose of NAD^+ from the α face of the ribose ring (Sauve et al., 2001; Sauve and Schramm, 2003) (Figures 1C and 2A). For these reasons, and because of the extensive direct contacts with conserved residues, we refer to this as the productive complex with NAD^+.

The NAD^+ in the productive complex forms extensive contacts with invariant residues in the C pocket (Figures 2B and 3). The C pocket was previously postulated to be important for catalysis (Min et al., 2001) but was found in structures of the Sir2Af1 enzyme bound to NAD^+ to be too far from the inferred position of the nicotinamide ring to account for the role of these residues in enzyme activity. In the productive complex of Sir2Af2 bound to NAD^+, a set of hydrophobic contacts with invariant residues mediate binding to the nicotinamide ring (Figures 2A and 2B). The invariant Gly23-Ala24-Gly25 motif forms a tight turn that inserts between the nicotinamide and associated ribose, placing the alanine methyl in van der Waals contact with one face of the nicotinamide ring. Additional contacts with Ile32, Phe35, and Asn101 help bury the nicotinamide ring in a largely hydrophobic environment within the C pocket. The carbonyl oxygen of the carboxamide group of nicotinamide forms direct hydrogen bonds with the backbone NH of Ile102, and the carboxamide amino group hydrogen bonds with the side chain of Asp103. This configuration can only be accommodated by rotating the nicotinamide carboxamide group about 150° from its preferred conformation (Bell et al., 1997; Olsen et al., 2003). The Asp103 side chain is further buttressed by van der Waals packing against the side chain of Leu105 and hydrogen bonds with Ser27 and the backbone amide of Leu105. Mutations of residues corresponding to Asp103 and Ser27 have been shown to abrogate both the deacetylation and nicotinamide exchange activity of sirtuins (Armstrong et al., 2002; Chang et al., 2002; Imai et al., 2000; Landry et al., 2000; Min et al., 2001). The nicotinamide ribose similarly forms direct contacts with invariant side chains. Gln100 hydrogen bonds with the 3′ hydroxyl of the ribose, while the 2′ hydroxyl hydrogen bonds to Asn101 (Figures 2A and 2B). The invariant Ser193 hydrogen bonds to the adenine phosphate and interacts with the Arg36 side chain, which wraps around the diphosphate of NAD^+ like a belt. Additionally, the backbone amides from Phe35 and Ala24 form direct hydrogen bonds with the nicotinamide and adenine phosphates, respectively. In summary, direct contacts with the productive conformation of NAD^+ account for the conservation of the most highly invariant motifs (GAGXS, GIPXFR, and TQNIDXL) in sirtuins (Figure 3).

The conformation of the NAD^+ in the productive complex differs from what would be expected from a low-energy state of the molecule. Both of the productive complexes contain distortions on the nicotinamide that bend the glycosidic bond and break its coplanarity with the nicotinamide ring. When the structure is refined using standard molecular constraints on NAD^+, the distortion on the ring and glycosidic bond produces a deviation of 8° from planarity; reducing the constraints to 1/10 of the standard values increases the distortion to about 15°. Importantly, the identical distortion was observed for the two crystallographically independent productive complexes but not at all for the NAD^+ in the nonproductive complex described below. Finally, the carboxamide group of the nicotinamide bound in the C pocket is rotated by about 150° from the most commonly observed position (Olsen et al., 2003). These factors, along with the burial of the charge of the nicotinamide ring in a largely hydrophobic environment, suggest a destabilization of the ground state of NAD^+ in the productive complexes.

Nonproductive Binding of NAD^+

The other type of Sir2Af2-NAD^+ complex in the crystal contains NAD^+ bound in a conformation that differs from the productive complexes (Figure 1B). In this complex, the N-ribose of NAD^+ binds near the acetyl-lysine binding tunnel, and the nicotinamide projects outside the enzyme cleft. This NAD^+ conformation would not permit simultaneous binding of acetyl-lysine to the enzyme in the manner seen in the Sir2Af2-peptide complex structure (Avalos et al., 2002) and places the N-ribose in the wrong orientation for an attack on the C1′ atom (Figure 1B). We therefore refer to this as a nonproductive complex with NAD^+. In contrast with the productive complexes, the nonproductive NAD^+ complex does not contain PEG bound within the acetyl-lysine binding tunnel. The conformations of NAD^+ in the previously described Sir2Af1-NAD^+ complexes (Min et al., 2001) differ from either conformation observed here and do not appear to represent catalytically competent complexes. These NAD^+ conformations do not place the nicotinamide within the C pocket and are incompatible with acetyl-lysine binding as deduced from structure superpositions (Figure 1B).

Conformational Differences among Sir2Af2 Complexes

A comparison of the structure of the Sir2Af2 apoenzyme, the Sir2Af2-ADP-ribose complex, the productive and nonproductive Sir2Af2-NAD^+ complexes, and the previously reported Sir2Af2-peptide complex (Avalos et al., 2002) reveals a large degree of conformational differences in the Sir2Af2. These six crystallographically

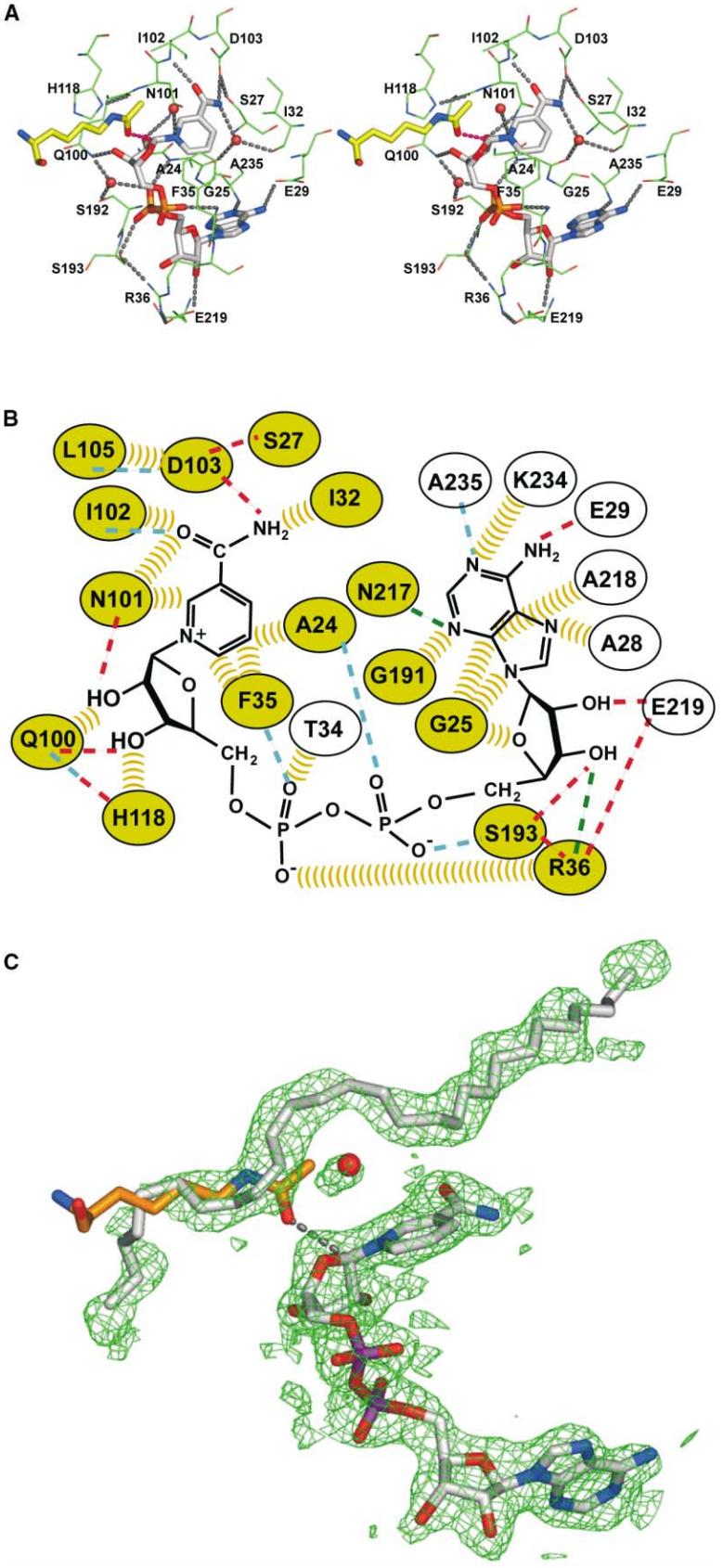

Figure 2. Productive Binding of NAD$^+$ to Sir2

(A) Stereo figure of the productive conformation of NAD$^+$ (white) bound to Sir2Af2 (green) and water (red spheres), with the nicotinamide ring in the C pocket. The superimposed acetyl-lysine from the structure of Sir2Af2-peptide is shown (yellow).

(B) Schematic diagram of the interactions between the protein and NAD$^+$ in the productive conformation. Highly conserved residues of Sir2 interacting with NAD$^+$ are shown in yellow circles. Van der Waals interactions are shown as yellow tracks. Dotted lines represent electrostatic interactions (green), hydrogen bonds with amino acid side chains (red), or hydrogen bonds with amino acid backbones (blue).

(C) Simulated annealing $F_o - F_c$ omit map (2.5σ) of the productive NAD$^+$ and bound PEG (white) superimposed with the acetyl-lysine from the structure of Sir2Af2 bound to peptide (yellow). A water molecule held by the PEG is shown (red sphere).

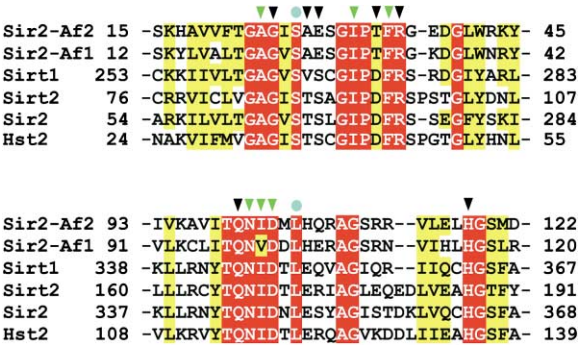

Figure 3. Functional Role of Conserved Residues in Sirtuins

Highly conserved (red) and conserved (yellow) residues are shown for six sirtuins. Residues contacting NAD^+ are marked by triangles; green triangles show residues in the C pocket that make specific contacts with NAD^+ in the productive conformation. Residues important to orient Asp103 in the C pocket are shown with blue circles.

independent structures make clear that there is significant conformational flexibility between the two subdomains of the enzyme (Figure 1D). In addition, amino acids 30–39 that contain residues that form the C pocket show a particularly high conformational flexibility, as has also been noted in other sirtuin structures (Finnin et al., 2001; Min et al., 2001; Zhao et al., 2003a, 2003b). Interestingly, the only two Sir2Af2 structures that are nearly superimposable are the two productive Sir2Af2-NAD^+ complexes (Figure 1D). Since these were crystallographically independent, their high degree of structural similarity suggests that the simultaneous binding of NAD^+ with nicotinamide in the C pocket, together with binding of a substrate mimic within the acetyl-lysine binding tunnel, may favor a particular enzyme conformation.

Discussion

Our results suggest a mechanism for NAD^+-dependent deacetylation by the Sir2 family of enzymes that accounts for the role of many of the key conserved residues in the enzyme active site (Figure 4). It is clear from this and previous work (Min et al., 2001) that NAD^+ can bind sirtuins in many different conformations. Most of these are incompatible with acetyl-lysine binding and enzyme chemistry, except for the productive conformation of NAD^+. Productive binding of NAD^+, which includes insertion of the nicotinamide ring into the C pocket, appears to be induced by the binding of an acetyl-lysine substrate, in agreement with a proposal by Min et al. (2001). Occupation of the acetyl-lysine binding tunnel likely promotes binding of NAD^+ in the C pocket by precluding alternate modes of NAD^+ binding. In support of this, we find that both of the crystallographically independent productive complexes contain PEG bound in the acetyl-lysine binding tunnel, whereas the nonproductive complex does not. This finding is reminiscent of an observation in the structure of the Rubisco large subunit SET domain methyl-transferase, where a molecule of the buffer HEPES mimics the binding of the lysine substrate to the enzyme (Trievel et al., 2002). The different structures of Sir2Af2 bound to NAD^+ with and without PEG suggest that the nonproductive conformations are energetically favored in the absence of bound acetylated peptide and that peptide binding causes the NAD^+ to shift into a higher-energy conformation that is catalytically competent and correctly positioned for nucleophilic attack by the acetyl-lysine.

The interactions of nicotinamide with the C pocket in the productive conformation of NAD^+ suggests that ground state destabilization of NAD^+ favors the initial nucleophilic attack on the N-ribose. In the productive complex induced by acetyl-lysine binding, the positive charge of the nicotinamide ring is buried in a largely hydrophobic environment, while the single polar group in the C pocket (Asp103) is hydrogen bonded to the nicotinamide carboxamide and is too distant to stabilize the charge on the ring. In addition, the productive complex contains distortions on the nicotinamide that bend the glycosidic bond and break the coplanarity of the ring. The rotation of the carboxamide group of the nicotinamide by about 150° from the most commonly observed position (Olsen et al., 2003), the result of hydrogen bonding interactions in the C pocket, are also likely to contribute to ground state destabilization of NAD^+. Together, these energizing effects would be expected to increase the electrophilicity of the nicotinamide ring nitrogen and hence the lability of the glycosidic bond, thereby enabling a weak nucleophile, like the acetyl-carbonyl oxygen, to function in the reaction. Nicotinamide binding in the C pocket also exposes the α face of the N-ribose to the acetyl-lysine substrate that is bound in a hydrophobic tunnel. The distance and orientation between the C1′ carbon of the N-ribose and the carbonyl oxygen of the acetyl-lysine suggests a substantially associative mechanism (SN2), which is also consistent with the absence of a negatively charged residue in the vicinity of the N-ribose that could stabilize the riboxocarbenium ion that would be produced in a mostly dissociative mechanism (SN1). The product of the attack of the carbonyl oxygen of acetyl-lysine on the C1′ carbon on the α face of the N-ribose is a high energy α-*O*-alkylamidate intermediate, to which the positive charge of the cleaved nicotinamide has migrated. The hydrophobic environment of the acetyl-lysine binding tunnel protects this intermediate from the solvent and maintains the high energetic state and high electrophilicity of the buried charge. In this manner, the α-*O*-alkylamidate is locked between the acetyl-lysine binding tunnel and the A and B pockets of the NAD^+ binding cleft, now presenting the β face of the ribose to the C pocket, which can bind and exchange nicotinamide with the solvent. At this point, the deacetylation reaction can proceed via the activation of the 2′ hydroxy oxygen of the ribose by the conserved His118 acting as a base. Alternatively, a nicotinamide molecule bound in the C pocket can do a reverse attack on the β face of the α-*O*-alkylamidate intermediate, on the C1′ carbon of the ribose, to reform β-NAD^+ in what is called the nicotinamide exchange reaction (Figure 4).

Comparison of the Sir2Af2-ADP-ribose complex with previous structures containing ADP-ribose or *O*-acetyl-ADP-ribose (Chang et al., 2002, Zhao et al., 2003b) suggests how some conserved residues may help stabilize and shield the *O*-alkylamidate intermediate from water,

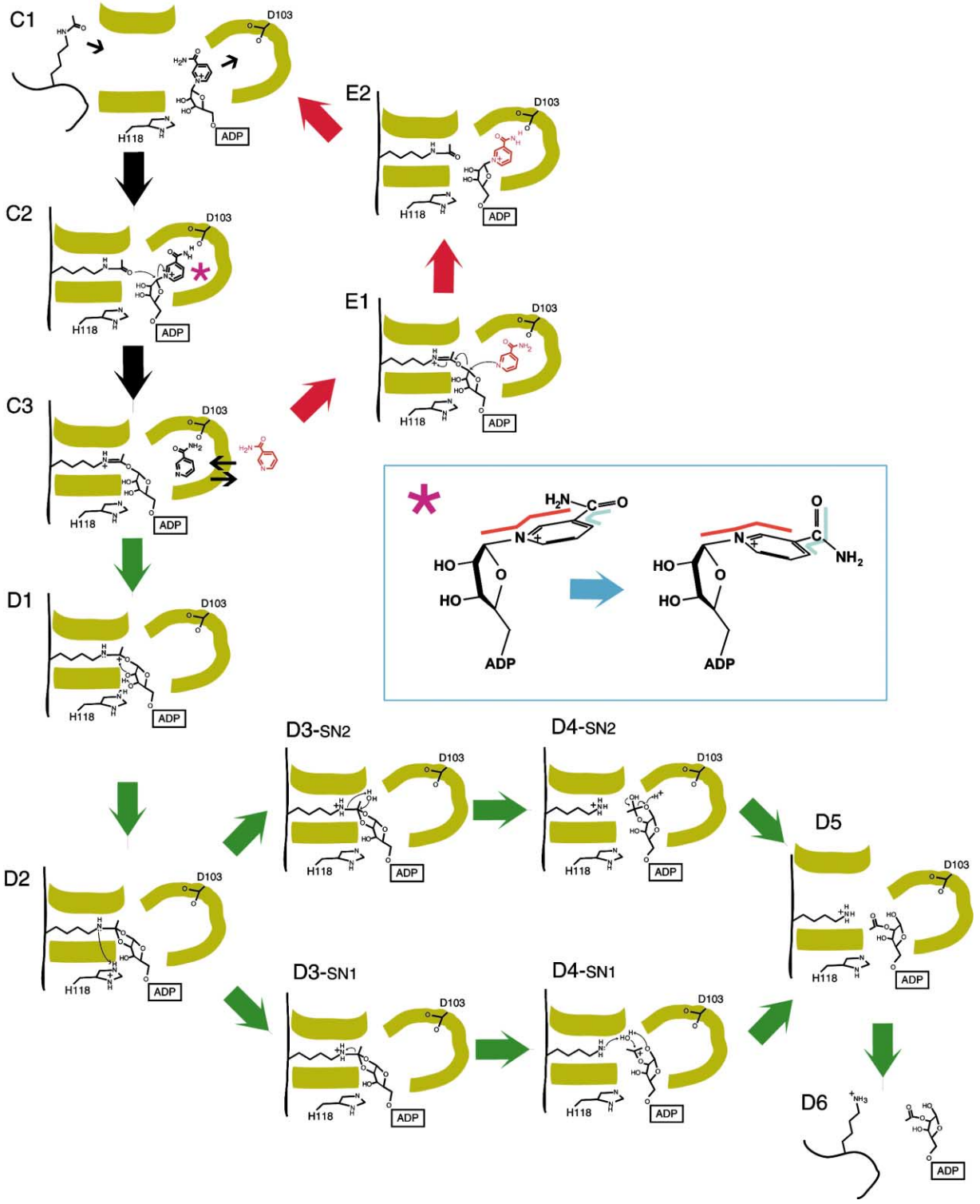

Figure 4. Structure-Based Mechanism of Sirtuins

Black arrows show common steps in the deacetylation and nicotinamide exchange reactions, red arrows show the nicotinamide exchange pathway, and green arrows show the deacetylation pathway. (C1) NAD^+ binds in an energetically favored nonproductive state in the absence of acetyl-lysine (Aly). The Aly binding tunnel is open (horizontal yellow bars). (C2) Aly binds, causes the Aly-binding tunnel to close, and induces the NAD^+ to shift into a destabilized and productive conformation due to strain and charge burial in the C pocket (yellow inverted C shape). The box (asterisk) illustrates the strain induced in the planarity of the glycosidic bond with the nicotinamide ring (red dihedral angle) and carboxamide group (blue dihedral angle). The resulting destabilization facilitates the mostly SN2 attack of the Aly carbonyl oxygen on the C1′ of the ribose, thereby breaking the glycosidic bond. (C3) The products of the attack are nicotinamide, free to exchange with the solvent, and a high-energy *O*-alkylamidate intermediate that preserves the energized state of the positive charge through burial in the Aly

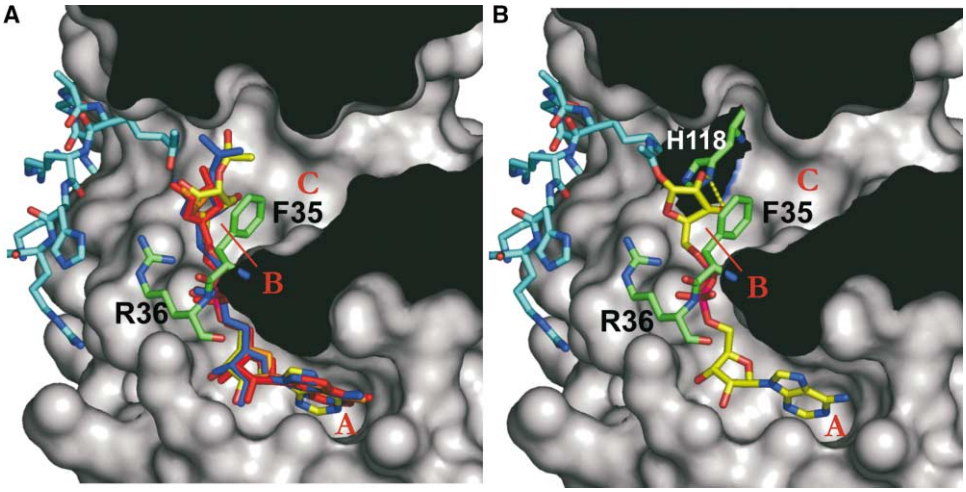

Figure 5. Binding of Nucleotide Products and Proposed High-Energy Intermediate

(A) The acetylated histone peptide (cyan) and 2′*O*-acetyl-ADP-ribose (yellow) from the ternary complex with Hst2 superimposed to the structures of ADP-ribose bound to Af2Sir2 (red) and Af1Sir2 (orange) as well as the structure of 2′*O*-acetyl-ADP-ribose bound to Af1Sir2 (dark blue). The A, B, and C pockets of Sir2Af2 are labeled in red.

(B) Proposed conformation of the bound *O*-alkylamidate intermediate, stabilized by Phe35 and Arg36 and in proper orientation for base activation by His118. The A, B, and C pockets of Sir2Af2 are labeled in red.

thereby preventing premature hydrolysis that would abort the reaction. All sirtuin structures containing ADP-ribose or *O*-acetyl-ADP-ribose have a high degree of similarity in the position of the N-ribose as well as its interactions with the invariant Phe35 and Arg36 (Sir2Af2 numbering) (Figure 5A). Interestingly, the carbonyl oxygen of the acetyl-lysine and the C1′ of the N-ribose in the ternary complex of Hst2 with *O*-acetyl-ADP-ribose and acetylated peptide (Zhao et al., 2003b) have the orientation expected in the *O*-alkylamidate intermediate of the reaction. We propose that the geometry of this ternary complex of Hst2 may resemble that of the *O*-alkylamidate intermediate and that Phe35 and Arg36 may play an important role in stabilizing the intermediate and shielding it from the solvent by adopting the positions that are consistently observed in all structures containing ADP-ribose or *O*-acetyl-ADP-ribose (Figure 5B). Furthermore, this orientation puts the N-ribose of the high-energy intermediate in an appropriate position to have its 2′ oxygen activated by His118 (Figure 5B). Phe35 and Arg36 undergo significant conformational shifts from their productive NAD^+-bound positions, to those in which the enzyme is bound to ADP-ribose, *O*-acetyl-ADP-ribose, and probably the *O*-alkylamidate intermediate. It seems that once the nicotinamide is cleaved and released, Phe35 is freed to rotate and stack against the β face of the α-*O*-alkylamidate intermediate and shield it from the solvent. Similarly, Arg36 moves from its belt-like conformation in the productive NAD^+ bound state to a position in which it interacts directly with the O4′ of the N-ribose where it may help stabilize and protect the high-energy intermediate. In the structure reported by Zhao et al. as a complex of Hst2 with NAD^+ (Zhao et al., 2003b), we observe a N-ribose and protein conformation very similar to the complex of Sir2Af2 with ADP-ribose and find compelling evidence that this complex of Hst2 (Zhao et al., 2003b) actually contains ADP-ribose. The nicotinamide ring in this structure is not visible and the ribose anomer could not be ascertained, raising the possibility noted by the authors (Zhao et al., 2003b) that the molecule could be either NAD^+ or ADP-ribose. However, the proximity of Tyr52 of Hst2 to the β face of the N-ribose, which would clash with a nicotinamide ring, together with the similarity of the Hst2 binary complex with other sirtuin ADP-ribose and *O*-acetyl-ADP-ribose complexes, suggests that the reported Hst2 complex contains ADP-ribose and not NAD^+. The N-ribose in the ADP-ribose complex is in a conformation that could not be adopted by NAD^+ and therefore argues against the conclusion by Zhao et al. that NAD^+ does not undergo a conformational change during catalysis (Zhao et al., 2003b).

Comparison of the structures reported here sheds light on the mechanism of nicotinamide exchange, an

binding tunnel. (D1) His118, acting as a base, activates the 2′OH for internal attack on the destabilizing charge, which cleaves the *O*-alkylamidate. (D2) The product of this attack is a cyclic amino-acetal that needs to be protonated to proceed with the reaction in two possible mechanisms: SN1 or SN2. (D3-SN1) The amino group leaves the intermediate, thereby cleaving the amide bond and producing a cyclic acyl-oxonium ion. (D4-SN1) The lysine is protonated and the acyl-oxonium is hydrolized to produce 2′O-acetyl-ADP-ribose. (D3-SN2) Water attacks the amino-acetal intermediate to produce deacetylated lysine and a cyclic orthoester. (D4-SN2) In an acid-catalyzed reaction, the cyclic orthoester is hydrolyzed to produce 2′O-acetyl-ADP-ribose. (D5) The positive charge in the lysine lacking other covalent bonds causes the Aly binding hydrophobic tunnel to open. (D6) As the Aly binding tunnel opens, the enzyme releases the deacetylated peptide. (E1, E2) The deacetylation reaction can be aborted at step C3 through rebinding of free nicotinamide, which can react with the *O*-alkylamidate intermediate and reverse the reaction, yielding NAD^+ and the acetylated peptide.

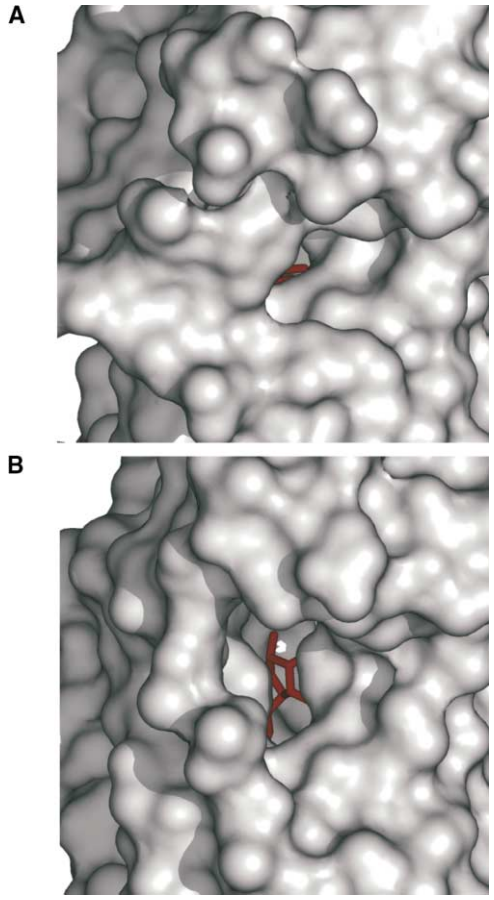

Figure 6. Surface Representation Showing the Putative Nicotinamide Exchange Tunnel

(A) The tunnel in the productive Sir2Af2-NAD$^+$ is relatively closed. (B) In contrast, the tunnel in the Sir2Af2-ADP ribose complex is significantly wider.

Table 1. Crystallographic Statistics

Diffraction Data	
Space group	$P2_12_12$
Unit cell (Å)	104.9, 181.6, 78.92
Resolution (Å)	2.3
Measured reflections	650,116 (58,315)
Unique reflections	67,550 (6662)
Completeness (%)	99.7 (99.0)
Average I/σ (merged data)	15.5 (4.5)
Multiplicity	9.6 (8.8)
Mosaicity	0.4
R_{sym}[a] (%)	10.9 (46.2)
Refinement Statistics	
Resolution range (Å)	30.0–2.3
Reflections (I/$\sigma > 0$)	67,462
Working set	64,042
Test set (5.0%)	3420
Total atoms	10,193
Protein atoms	9542
NAD$^+$ atoms	132
ADP-ribose atoms	36
Zn^{2+} atoms	9
PEG atoms	101
Sulfate atoms	60
Water molecules	313
R_{factor}[b] (%)	20.7
R_{free}[c] (%)	25.0
B factor (Å^2)	40.3
Rms deviations	
Bond lengths (Å)	0.009
Bond angles (°)	1.32

Values in parentheses correspond to the highest-resolution shell, 2.38–2.30 Å.

[a] $R_{sym} = \Sigma|I - \langle I\rangle|/\Sigma I$, where I is the observed intensity and $\langle I\rangle$ the average intensity of multiple observations of symmetry-related reflections.

[b] $R_{factor} = \Sigma||F_o| - |F_c||/\Sigma|F_o|$, where F_o is the amplitude of the observed structure factor and F_c is the structure factor calculated from the model.

[c] R_{free} is the R_{factor} calculated with 5% of the reflection data randomly omitted from the refinement.

important competing reaction (Sauve and Schramm, 2003) that regulates sirtuin activity in response to cellular nicotinamide levels (Bitterman et al., 2002). Nicotinamide exchange must occur after the nicotinamide is cleaved from NAD$^+$, while the enzyme remains bound to the *O*-alkylamidate intermediate. Superposition of the five Sir2Af2 structures reported here and the previously reported Sir2Af2-peptide structure reveals a remarkable degree of flexibility in the Sir2 structure that might facilitate such exchange (Figure 1D). The flexible loop region that forms one wall of the C pocket is highly mobile or disordered in all Sir2 structures except in the productive complexes of Sir2Af2. The mobility of this portion of the nicotinamide binding pocket, together with gross motions of the small domain of the enzyme, might allow the cleaved nicotinamide to exit the enzyme and a second nicotinamide to bind the C pocket in two possible ways. The wall of the C pocket may disassemble upon NAD$^+$ cleavage to release and recapture nicotinamide. Alternatively, nicotinamide might exchange in and out of the enzyme through a channel that communicates the C pocket to the solvent on the other side of the protein (Figures 1B and 1C), which is present in all six structures of Sir2Af2, sometimes empty and other times occupied by a PEG molecule. Interestingly, this channel can contract and expand as another consequence of the flexibility of the small domain of the enzyme (Figure 6). This channel is also present in the human SirT1 and yeast Hst2 enzymes, and, although it has not been seen in the Sir2Af1 enzyme, we speculate that a similar channel might form in certain conformations of this enzyme.

Our proposed reaction mechanism involving activation of NAD$^+$ via ground state destabilization resembles the mechanism of activation of deoxyuridine by uracil-DNA glycosylase (UDG), an enzyme that cleaves the glycosidic bond of deoxyuridine misincorporated into DNA (Parikh et al., 2000). UDG transfers its DNA binding energy into catalytic power by stretching the glycosidic bond and distorting its planarity with the uracil ring, which further weakens it by a combination of the anomeric and σ-π_{Arom} effects (Parikh et al., 2000). The distortion of the nicotinamide ring of NAD$^+$ in its productive conformation with Sir2Af2 is very similar to that observed in the deoxyuridine analog 2′-deoxypseudouridine (dΨU) bound to UDG (Parikh et al., 2000). By analogy to UDG, sirtuins likely transfer the energy of binding of the acetylated peptide into the activation of the glyco-

sidic bond by deforming its planarity with the nicotinamide and burying the positive charge of the nicotinamide in a largely hydrophobic environment. The instability generated by the buried charges in either the C pocket (in the form of NAD^+) or the hydrophobic tunnel (in the form of the *O*-alkylamidate intermediate) may be essential to catalyze the forward (*O*-alkylamidate formation) and reverse (nicotinamide exchange) reactions, respectively. The uncommitted condition of the enzyme bound to the high-energy *O*-alkylamidate intermediate accounts for the sensitivity of sirtuins to the concentration of nicotinamide and is probably the basis for their regulation via nicotinamide exchange. Charge destabilization initiates with the productive binding of NAD^+ in the C pocket, which is likely induced by substrate binding, and is not relieved until product release, when the charge is transferred to the deacetylated lysine and causes the opening of the hydrophobic tunnel (Figure 4). Therefore, the instability resulting from charge burial in these enzymes and its relief through product release seem to be the global driving force of NAD^+-dependent deacetylation by Sir2 proteins.

Experimental Procedures

Crystallization of Sir2Af2 with NAD^+ and ADP Ribose

The Sir2Af2 protein from *A. fulgidus* was expressed in *E. coli* and purified as described previously (Smith et al., 2002). The protein was dialyzed into 10 mM HEPES (pH 7.4) with 1 mM TCEP and concentrated to 20 mg/ml. To 50 μl of the protein solution, we added 5.5 μl of 100 mM NAD^+ solution, freshly made and neutralized to pH 7 with 1 N NaOH, to a final concentration of 10 mM NAD^+. This solution was incubated for 30 min at room temperature before setting crystallization trays. Crystals were grown by the hanging drop method in 0.1 M HEPES (pH 7.4), 1.8 M ammonium sulfate, and 1% PEG400 at 20°C. Crystals appeared in 2–5 days and grew in size for approximately 10 days, at which point they were flash frozen in nujol oil and stored in liquid nitrogen until use. The crystals formed in space group $P2_12_12$ with unit cell dimensions a = 104.9 Å, b = 181.6 Å, and c = 78.9 Å and contain five molecules in the asymmetric unit.

Structure Determination

Diffraction data were collected at beam line X25 of the NSLS at BNL and reduced with HKL2000 (Otwinowski and Minor, 1997). The structure was solved by molecular replacement using MOLREP (Vagin and Teplyakov, 1997). The search model was the structure of Sir2Af2 in the complex with acetylated p53 peptide (accession number 1MA3) with the p53 peptide removed and the enzyme broken into two segments: the Rossmann fold domain and the small domain. The structures of the five molecules were built independently using O (Jones et al., 1991) and Xfit (McRee, 1999) and refined with simulating annealing and energy minimization in CNS (Brunger et al., 1998), without any noncrystallographic symmetry constraints. The five structures were treated independently throughout the refinement. The positions of the NAD^+ and PEG molecules, as well as flexible regions in the proteins, were ascertained with simulated annealing omit maps using CNS. Some protein regions showed poor electron density definition, suggesting areas of high disorder or flexibility, including residues 34–40 and 70–74 of molecule A (nonproductive complex); residues 72–77 of molecules C (one of the productive complexes) and D (apo-enzyme); and residues 144–147 and 209–212 of molecule E (ADP-ribose complex). Residues 29–39 in molecule D and 73 and 74 in molecule E could not be interpreted in the omit map and were therefore not included in the model. The final model contains five Sir2Af2 monomers, three molecules of NAD^+, one of ADP ribose, eight of PEG, nine zinc atoms, twelve sulfates, and 313 waters. The crystallographic statistics are summarized in Table 1. The global superposition of Figure 1D was done by minimizing the distance between the backbone Cα atoms in the β sheet of the Rossmann fold domain of the structures. The active site superpositions in Figures 1B, 1C, 2A, 2C, and 5 were done by minimizing the distance between the backbone Cα atoms of residues 23–25, 99–103, 105, and 118.

Acknowledgments

We thank K. Witwer for help in growing crystals; M. Amzel, M. Bianchet, I. Celic, P. Cole, S. Gabelli, B.Garcia-Moreno, A. Gittis, J. Lorsch, A. Mildvan, and members of the Wolberger lab for helpful discussions; and Michael Becker from Beamline X25 at the Brookhaven National Synchrotron Light Source. Supported by the National Institutes of Health (GM62385).

Received: December 11, 2003
Revised: January 16, 2004
Accepted: January 22, 2004
Published: March 11, 2004

References

Anderson, R.M., Bitterman, K.J., Wood, J.G., Medvedik, O., and Sinclair, D.A. (2003). Nicotinamide and PNC1 govern lifespan extension by calorie restriction in Saccharomyces cerevisiae. Nature *423*, 181–185.

Armstrong, C.M., Kaeberlein, M., Imai, S.I., and Guarente, L. (2002). Mutations in Saccharomyces cerevisiae gene SIR2 can have differential effects on in vivo silencing phenotypes and in vitro histone deacetylation activity. Mol. Biol. Cell *13*, 1427–1438.

Avalos, J.L., Celic, I., Muhammad, S., Cosgrove, M.S., Boeke, J.D., and Wolberger, C. (2002). Structure of a Sir2 enzyme bound to an acetylated p53 peptide. Mol. Cell *10*, 523–535.

Bell, C.E., Yeates, T.O., and Eisenberg, D. (1997). Unusual conformation of nicotinamide adenine dinucleotide (NAD) bound to diphtheria toxin: a comparison with NAD bound to the oxidoreductase enzymes. Protein Sci. *6*, 2084–2096.

Bitterman, K.J., Anderson, R.M., Cohen, H.Y., Latorre-Esteves, M., and Sinclair, D.A. (2002). Inhibition of silencing and accelerated aging by nicotinamide, a putative negative regulator of yeast sir2 and human SIRT1. J. Biol. Chem. *277*, 45099–45107.

Braunstein, M., Rose, A.B., Holmes, S.G., Allis, C.D., and Broach, J.R. (1993). Transcriptional silencing in yeast is associated with reduced nucleosome acetylation. Genes Dev. *7*, 592–604.

Brunger, A.T., Adams, P.D., Clore, G.M., DeLano, W.L., Gros, P., Grosse-Kunstleve, R.W., Jiang, J.S., Kuszewski, J., Nilges, M., Pannu, N.S., et al. (1998). Crystallography & NMR system: a new software suite for macromolecular structure determination. Acta Crystallogr. D Biol. Crystallogr. *54*, 905–921.

Chang, J.H., Kim, H.C., Hwang, K.Y., Lee, J.W., Jackson, S.P., Bell, S.D., and Cho, Y. (2002). Structural basis for the NAD-dependent deacetylase mechanism of Sir2. J. Biol. Chem. *277*, 34489–34498.

Finnin, M.S., Donigian, J.R., and Pavletich, N.P. (2001). Structure of the histone deacetylase SIRT2. Nat. Struct. Biol. *8*, 621–625.

Fulco, M., Schiltz, R.L., Iezzi, S., King, M.T., Zhao, P., Kashiwaya, Y., Hoffman, E., Veech, R.L., and Sartorelli, V. (2003). Sir2 regulates skeletal muscle differentiation as a potential sensor of the redox state. Mol. Cell *12*, 51–62.

Gottlieb, S., and Esposito, R.E. (1989). A new role for a yeast transcriptional silencer gene, SIR2, in regulation of recombination in ribosomal DNA. Cell *56*, 771–776.

Imai, S., Armstrong, C.M., Kaeberlein, M., and Guarente, L. (2000). Transcriptional silencing and longevity protein Sir2 is an NAD-dependent histone deacetylase. Nature *403*, 795–800.

Jackson, M.D., Schmidt, M.T., Oppenheimer, N.J., and Denu, J.M. (2003). Mechanism of nicotinamide inhibition and transglycosidation by Sir2 histone/protein deacetylases. J. Biol. Chem. *278*, 50985–50998.

Jones, T.A., Zou, J.Y., Cowan, S.W., and Kjeldgaard (1991). Improved methods for building protein models in electron density

maps and the location of errors in these models. Acta Crystallogr. A *47*, 110–119.

Kaeberlein, M., McVey, M., and Guarente, L. (1999). The SIR2/3/4 complex and SIR2 alone promote longevity in Saccharomyces cerevisiae by two different mechanisms. Genes Dev. *13*, 2570–2580.

Landry, J., Sutton, A., Tafrov, S.T., Heller, R.C., Stebbins, J., Pillus, L., and Sternglanz, R. (2000). The silencing protein SIR2 and its homologs are NAD-dependent protein deacetylases. Proc. Natl. Acad. Sci. USA *97*, 5807–5811.

Lin, S.J., Defossez, P.A., and Guarente, L. (2000). Requirement of NAD and SIR2 for life-span extension by calorie restriction in Saccharomyces cerevisiae. Science *289*, 2126–2128.

Luo, J., Nikolaev, A.Y., Imai, S., Chen, D., Su, F., Shiloh, A., Guarente, L., and Gu, W. (2001). Negative control of p53 by Sir2alpha promotes cell survival under stress. Cell *107*, 137–148.

McRee, D.E. (1999). XtalView/Xfit—a versatile program for manipulating atomic coordinates and electron density. J. Struct. Biol. *125*, 156–165.

Min, J., Landry, J., Sternglanz, R., and Xu, R.M. (2001). Crystal structure of a SIR2 homolog-NAD complex. Cell *105*, 269–279.

Muth, V., Nadaud, S., Grummt, I., and Voit, R. (2001). Acetylation of TAF (I)68, a subunit of TIF-IB/SL1, activates RNA polymerase I transcription. EMBO J. *20*, 1353–1362.

North, B.J., Marshall, B.L., Borra, M.T., Denu, J.M., and Verdin, E. (2003). The human Sir2 ortholog, SIRT2, is an NAD+-dependent tubulin deacetylase. Mol. Cell *11*, 437–444.

Olsen, R.A., Liu, L., Ghaderi, N., Johns, A., Hatcher, M.E., and Mueller, L.J. (2003). The amide rotational barriers in picolinamide and nicotinamide: NMR and ab initio studies. J. Am. Chem. Soc. *125*, 10125–10132.

Otwinowski, Z., and Minor, W. (1997). Processing of X-ray diffraction data collected in oscillation mode. Methods Enzymol. *276*, 307–326.

Parikh, S.S., Walcher, G., Jones, G.D., Slupphaug, G., Krokan, H.E., Blackburn, G.M., and Tainer, J.A. (2000). Uracil-DNA glycosylase-DNA substrate and product structures: conformational strain promotes catalytic efficiency by coupled stereoelectronic effects. Proc. Natl. Acad. Sci. USA *97*, 5083–5088.

Sauve, A.A., and Schramm, V.L. (2003). Sir2 regulation by nicotinamide results from switching between base exchange and deacetylation chemistry. Biochemistry *42*, 9249–9256.

Sauve, A.A., Celic, I., Avalos, J., Deng, H., Boeke, J.D., and Schramm, V.L. (2001). Chemistry of gene silencing: the mechanism of NAD+-dependent deacetylation reactions. Biochemistry *40*, 15456–15463.

Smith, J.S., Brachmann, C.B., Celic, I., Kenna, M.A., Muhammad, S., Starai, V.J., Avalos, J.L., Escalante-Semerena, J.C., Grubmeyer, C., Wolberger, C., et al. (2000). A phylogenetically conserved NAD+-dependent protein deacetylase activity in the Sir2 protein family. Proc. Natl. Acad. Sci. USA *97*, 6658–6663.

Smith, J.S., Avalos, J., Celic, I., Muhammad, S., Wolberger, C., and Boeke, J.D. (2002). SIR2 family of NAD (+)-dependent protein deacetylases. Methods Enzymol. *353*, 282–300.

Starai, V.J., Celic, I., Cole, R.N., Boeke, J.D., and Escalante-Semerena, J.C. (2002). Sir2-dependent activation of acetyl-CoA synthetase by deacetylation of active lysine. Science *298*, 2390–2392.

Tanner, K.G., Landry, J., Sternglanz, R., and Denu, J.M. (2000). Silent information regulator 2 family of NAD-dependent histone/protein deacetylases generates a unique product, 1-O-acetyl-ADP-ribose. Proc. Natl. Acad. Sci. USA *97*, 14178–14182.

Tanny, J.C., and Moazed, D. (2001). Coupling of histone deacetylation to NAD breakdown by the yeast silencing protein Sir2: evidence for acetyl transfer from substrate to an NAD breakdown product. Proc. Natl. Acad. Sci. USA *98*, 415–420.

Tissenbaum, H.A., and Guarente, L. (2001). Increased dosage of a sir-2 gene extends lifespan in Caenorhabditis elegans. Nature *410*, 227–230.

Trievel, R.C., Beach, B.M., Dirk, L.M., Houtz, R.L., and Hurley, J.H. (2002). Structure and catalytic mechanism of a SET domain protein methyltransferase. Cell *111*, 91–103.

Vagin, A., and Teplyakov, A. (1997). MOLREP: an automated program for molecular replacement. J. Appl. Crystallogr. *30*, 1022–1025.

Vaziri, H., Dessain, S.K., Ng Eaton, E., Imai, S.I., Frye, R.A., Pandita, T.K., Guarente, L., and Weinberg, R.A. (2001). hSIR2 (SIRT1) functions as an NAD-dependent p53 deacetylase. Cell *107*, 149–159.

Zhao, K., Chai, X., Clements, A., and Marmorstein, R. (2003a). Structure and autoregulation of the yeast Hst2 homolog of Sir2. Nat. Struct. Biol. *10*, 864–871.

Zhao, K., Chai, X., and Marmorstein, R. (2003b). Structure of the yeast Hst2 protein deacetylase in ternary complex with 2′-O-acetyl ADP ribose and histone peptide. Structure *11*, 1403–1411.

Accession Numbers

Coordinates with accession number 1S7G have been deposited in the Protein Data Bank.